Published in final edited form as:
Cancer Lett. 2010 December 18; 299(1): 45–53. doi:10.1016/j.canlet.2010.08.002.

Nuclear Factor-κB Modulates Cellular Glutathione and Prevents Oxidative Stress in Cancer Cells

Qinghang Meng[a], **Zhimin Peng**[a,1], **Liang Chen**[a], **Jutong Si**[b], **Zhongyun Dong**[c], and **Ying Xia**[a,*]

[a]Department of Environmental Health, University of Cincinnati, College of Medicine, Cincinnati, Ohio 45267

[b]Human Biology Division, Fred Hutchinson Cancer Research Center, Seattle, WA 98109

[c]Department of Internal Medicine, University of Cincinnati, College of Medicine, Cincinnati, Ohio 45267

Abstract

The NF-κB is best known for its role in inflammation. Here we show that constitutive NF-κB activity in cancer cells promotes the biosynthesis of redox scavenger glutathione (GSH), which in turn confers resistance to oxidative stress. Inhibition of NF-κB significantly decreases GSH in several lines of human leukemia and prostate cancer cells possessing high or moderate NF-κB activities. Concomitantly, NF-κB inhibition by pharmacological and molecular means sensitizes "NF-κB positive" cancer cells to chemically-induced oxidative stress and death. We propose that inhibition of NF-κB can reduce intracellular GSH in "NF-κB-positive" cancers thereby improving the efficacy of oxidative stress-based anti-cancer therapy.

Keywords

NF-κB; glutathione; arsenic; leukemia; prostate cancer; oxidative stress

1. Introduction

The Nuclear Factor-κB (NF-κB) signaling pathway plays an important role in inflammation, cancer and stress responses. NF-κB comprises a group of transcription factors normally sequestered in the cytoplasm through binding to the so-called inhibitor of NF-κB (IκB). Activation of NF-κB by growth and inflammatory factors is mediated through the IκB kinases (IKKs), which phosphorylate IκB, resulting in IκBα ubiquitination and subsequent proteosome-dependent degradation. As a consequence, NF-κB is released from the IκB complex and translocates to the nucleus, where it binds to consensus NF-κB sites in DNA to

[*]**Corresponding author:** Ying Xia, Ph.D. Department of Environmental Health, College of Medicine, University of Cincinnati, 123 East Shields Street, Cincinnati, Ohio 45267-0056, Phone: (513)-558-0371, FAX: (513)-558-4397, ying.xia@uc.edu.
[1]**Current address:** Radiation Oncology Research Laboratory, University of Maryland, Bressler Research Building, 7-017, 655 West Baltimore St., Baltimore, MD 21201

Conflict of interest
The authors do not have any conflicts of interest associated with this manuscript.

activate gene expression [1]. The wide distribution of NF-κB binding sites in the genome allows NF-κB to regulate a vast number of genes and participate in fundamental cellular processes, such as proliferation, apoptosis and differentiation [1;2].

Some NF-κB targets, such as the cytochrome p450 CYP1B1, MnSOD, FHL and metallothionein, have been implicated in modulating cellular redox potential [3–6]. Recently, we showed that the NF-κB pathway is critical for maintaining the homeostatic levels of glutathione (GSH) [7]. Glutathione is an important intracellular protective antioxidant, responsible for hydrophilic scavenging of radicals and electrophiles and for maintaining the redox state of proteins. GSH *de novo* synthesis, carried out by the consecutive action of two ATP-dependent enzymes, γ-glutamate-cysteine ligase (γ-GCL) and GSH synthase (GS), primarily determines cellular GSH level [8]. γ-GCL is the rate-limiting enzyme, consisting of a heterodimer composed of a catalytic (γ-GCLC) and a regulatory subunit (γ-GCLM) [9]. We find that the IKKβ-NF-κB pathway is responsible for maintaining basal GCLC/GCLM expression, which in turn regulates GSH biosynthesis. Cells impaired in this pathway have low GSH contents and high sensitivity to damage caused by oxidative stress. These observations suggest that high NF-κB activities may confer greater redox potential and resistance to oxidative stress.

Compelling evidence indicates that constitutive activation or dysregulation of NF-κB is associated with many types of cancers. For example, constitutive NF-κB activity is detected in 80% of acute myeloid leukemia [10–13] and in prostate cancer cells [14;15]. Viral infection, cancer-associated chromosomal translocation and mutations that disrupt genes encoding components of the regulatory pathway, and uncoupling NF-κB factors from their regulators in tumor cells can all lead to NF-κB activation [16]. Autocrine and paracrine production of pro-inflammatory cytokines in the tumor microenvironment have also been shown to activate NF-κB. The NF-κB activity in turn is linked to several aspects of tumorigenesis, including promoting cancer-cell proliferation, preventing apoptosis, and increasing the angiogenic and metastatic potential of a tumor [2;16].

In the present studies, we tested the hypothesis that constitutive NF-κB activity in cancer cells can increase cellular glutathione and confer resistance to oxidative stress. We showed that several myeloid leukemia and prostate cancer cells had constitutive NF-κB activity. Inhibition of NF-κB significantly reduced GSH in the “NF-κB-positive” cancer cells and increased their sensitivity to oxidative stress damage. These observations suggest that down regulation of glutathione is a possible mechanism through which the NF-κB inhibitors potentiate the efficacy of oxidative stress-based anti-cancer therapies.

2. Materials and Methods

2.1. Cell culture reagents, antibodies and plasmids

Dulbecco’s Modification of Eagle’s medium (DMEM) was from Mediatech (Manassas, VA). Prostate Epithelial Cell Growth Medium (PrEGM) was from Lonza (Basel, Switzerland). Minimum Essential Medium Eagle (EMEM) was from ATCC Corp. All the other cell culture reagents, including RPMI 1640, Fetal Bovine Serum (FBS), and penicillin-streptomycin were from Invitrogen Corp (Carlsbad, CA).

The fibroblasts derived from mouse embryonic fibroblasts (MEFs) were provided by Dr. Michael Karin (University of California, San Diego) and cultured in DMEM supplemented with 10% FBS, 50 U/ml penicillin, and 50 mg/ml streptomycin. The Human Prostate Epithelial Cells (hPrEC) were maintained in PrEGM, following the manufacturer’s instruction. The prostate cancer cells used for this study included LNCaP, an androgen-sensitive human prostate adenocarcinoma cells, DU145 and PC-3, the androgen-insensitive

prostate cancer cell lines, and PC-3MM2, a highly metastatic PC3 derivative [17]. The prostate cancer cells were maintained in EMEM supplemented with 5% FBS, 50 U/ml penicillin, and 50 mg/ml streptomycin. The human promyelocytic leukemia cell NB4, KG1 and HL60R, a retinoic acid resistant sub-clone of HL-60 [18], chronic myelogenous leukemia cells K562GS and KCL22, myelomonocytic leukemia THP1 and thyroid cancer ML1 were maintained in RPMI 1640 supplemented with 10% FBS, 50 U/ml penicillin, 50 mg/ml streptomycin.

The NF-κB p65 inhibitor, JSH-23, was from Calbiochem-Novabiochem (San Diego, CA). Arsenic trioxide, sodium arsenite, *tert*-Butylhydroquinone (tBHQ), glutathione (GSH) and glutathione disulfide (GSSG) were from Sigma (St. Louis, MO). Luciferase reporter plasmids containing binding elements for NF-κB (NF-κB-luc), and the promoters of *Gclm* (*Gclm*-luc) and *Gclc* (*Gclc*-luc) were described previously [19–21]. The expression vector for β-galactosidase was from Fisher Scientifics (Pittsburgh, PA).

2.2. Cellular glutathione contents

The intracellular levels of GSH and GSSG were determined using the methods described previously [22]. Redox potentials at pH 7.0 were calculated as described [23] by inserting molar GSH and GSSG concentrations into the Nernst equation, $\Delta E'$ ($GSSG + 2H^+ \rightarrow 2GSH$) = $-240\ mV - (61.5\ mV/2e^-) \times \log([GSH]^2/[GSSG])$

2.3. Electrophoretic mobility shift assay (EMSA)

The NF-κB binding site oligonucleotide 5'-GATCGAGGGGACTTTCCCTAGC-3' and its complement were labeled using the Biotin 3'-End DNA Labeling Kit (Pierce Biotech) and annealed. Twenty fmole biotin-labeled probes were mixed with 10 μg nuclear extracts in the presence of 50 μg/ml poly (dI-dC), 5% glycerol, 0.05% NP-40, 5 mM $MgCl_2$ in binding buffer (10 mM Tris–HCl, pH 7.5, 50 mM KCl, 1 mM DTT). Following incubation for 20 min at room temperature, the DNA-protein complexes were separated in a 6 % non-denaturing polyacrylamide gel and transferred to a positively charged nylon membrane (Millipore, Bedford, MA). After UV cross-linking, the DNA-protein complex was detected using a streptavidin–horseradish peroxidase (HRP) conjugated antibody following the manufacturer's protocol (Pierce Biotech).

2.4. Transfection and luciferase reporter assay

Cells plated in 24-well tissue culture plates at 5×10^4 cells/well were grown for 24 h before transfection. Plasmid transfection was carried out using Lipofectamine Plus reagent (Invitrogen, Carlsbad, CA), 0.4 μg luciferase reporter and 0.1 μg β-galactosidase plasmids/well, following the manufacturer's instructions. Twenty-four hours after transfection, cells were subjected to the indicated treatments for 16 hours. Cells were lysed and luciferase activity and β-galactosidase activity were determined using the luciferase and β-galactosidase reporter kits (Promega, Madison, WI), according to the manufacturer's protocol. Relative luciferase versus β-gal activity was calculated.

The siGENOME SMARTpool siRNA against mouse and human *IKK*β gene and scrambled siRNA were from Dharmacon. The siRNA for IKKβ contains four siRNA: 5' GAAGAUACUUGAACCAGUU; 5' CCAAUAAUCUUAACAGUGU; 5' GAAGAUCGCCUGUAGCAAA; and 5' GUAAGACCGUGGUUUGUAA. The siRNA transfection was performed using HiperFect transfection reagent (QIAGEN, Hilden, Germany) with fast-forward transfection protocol. Briefly, 5×10^6 cells were seeded in a 10 cm plate containing 6 ml of regular culture medium, with an addition of 0.8 nmol siRNA (at a final 100 nM) and 200 μl transfection reagent in 2 ml DMEM. The cells were incubated under normal culture condition for 48 h before further treatment.

2.5. Reverse transcription and real-time PCR

Total RNA was extracted using Trizol reagent (Invitrogen, Carlsbad, CA) and was used for reverse transcription with random hexamer primers and the Stratascript enzyme, following the instructions from the manufacturer. The cDNA was subjected to quantitative PCR using an MJ research thermal cycler system and SYBER Green QPCR Master Mix (Stratagene, La Jolla, CA). The conditions for the PCR amplification were optimized for specific PCR reactions. At the end of the PCR the samples were subjected to melting curve analysis. All reactions were performed at least in triplicate. The primers used to amplify human cDNA were *IKK*β, 5' TGACAGTCAGGAAATGGTACGGCT and 5' ATTCATGCTATCCGGGCTTCCACT; and *GAPDH* 5' AAT GAC CCC TTC ATT GACC and 5' TGA AGA CAC CAG TAG ACT CC.

2.6. Cell apoptosis and survival

Cell viability was assessed using MTS assay. Briefly, cells grown on 96-well plate in 100 μl culture medium were incubate with 20 μl of CellTiter 96 AQ_{ueous} One Solution Cell Proliferation Assay (Promega, Madison, WI) for 1–4 hours at 37°C in a humidified, 5% CO_2 atmosphere. The absorbance at 490 nm was measured using a 96-well plate reader. The relative cell survival was calculated based on the absorbance values of each experimental condition. The absorbance in the absence of chemicals was set as 1.

Cell viability was also assessed using trypan blue staining assay. Briefly, the cells cultured on 96-well plate were incubated with 20μl 0.2% trypan blue solution for 3 minutes at room temperature. After removing the staining solution, the viable (trypan blue negative) and dead (trypan blue positive) cells were counted under a microscope. The relative survival was calculated by dividing the numbers of unstained cells by total cells. At least 500 cells under each treatment condition were observed.

TUNEL assay was performed using ApopTag Plus fluorescein In Situ Apoptosis Detection kit according to manufacturer's recommendation (Millipore, Temecula, CA). Briefly, cells cultured on cover slips were fixed by 4% paraformaldehyde in PBS and post-fixed in pre-cooled ethanol: acetic acid (2:1). The DNA fragments in apoptotic cells were labeled with the digoxigenin-tagged nucleotide and detected by a florescence conjugated anti-digoxigenin antibody. The nuclei were stained with DAPI. Images were taken under fluorescence microscopy and the percentage of apoptosis was calculated by dividing the number of TUNEL positive cells by that of total cells. At least 500 cells under each treatment condition were observed.

Cell apoptosis was also measured by Annexin-V-PE Apoptosis Detection Kit (BD Pharmingen, San Jose, CA). Briefly, cells were washed twice with cold PBS and resuspended in Binding Buffer at a concentration of 1×10^6 cells/ml. A total of 1×10^5 cells (100 μl) were incubated with 5 μl of Annexin V-PE and 5 μl of 7-ADD for 15 min at RT in the dark. The Annexin V-PE- and 7-AAD-labeling were detected by flow cytometry using excitation 488 nm, emission 578 nm for PE and 650 nm for 7-ADD. The Annexin V-PE positive and 7-AAD negative cells were recognized as apoptotic at early stage, whereas, the Annexin V-PE and 7-AAD positive cells were recognized as apoptotic at late stage.

2.7. DCF labeling

To measure intracellular H_2O_2, cells were incubated with 10 μM CM-H2DCFDA for 30 minutes. The DCF-positive cells were identified and quantified by flow cytometry at excitation 488 nm and emission 520–530 nm.

2.8 Calculate the median lethal concentration

The median lethal concentration (LC_{50}) was calculated using the probit analysis method.

2.9. Statistical analysis

Data represent the average ± SD from at least three independent experiments. Statistical comparisons were performed using analysis of variance (ANOVA) for repeated measurements followed by Student's two-tailed paired *t*-test. * represents statistical significance p value <0.05, ** p <0.01 and *** p <0.001.

3. Results

3.1. Constitutive NF-κB activities in leukemia cells confer arsenic resistance

Constitutive activation of NF-κB is associated most commonly with hematologic tumors and has implicated NF-κB in resistance to cancer chemotherapy [24]. To determine whether NF-κB was constitutively active in cancer cells, we examined NF-κB DNA binding activity by EMSA using nuclear extracts from leukemia cells (Fig. 1A). Among seven lines of leukemia cells, relatively strong DNA-binding activities were detected in K562GS and KG1, moderate activities in KCL22 and ML1, weak activities in NB4 and HL60R, and no detectable NF-κB activity in THP1. Using a less sensitive Western blotting measurement, we detected low levels of nuclear NF-κB p65 subunit in KG1 cells, but not in NB4 or THP1 cells (Fig. 1B). Our results are consistent with previously findings, showing variable levels of basal constitutive NF-κB activity in leukemia cells [25–28].

Arsenic trioxide has a powerful effect on inducing complete remission of acute promyelocytic leukemia (APL) and its therapeutic efficacy is attributed in part to the ability to induce cancer cell apoptosis [29;30]. To evaluate arsenic effects, we treated leukemia cells with low sub-therapeutical doses of arsenic and examined cell survival (Fig. 1C). Compared to control vehicle treated cells, NB4 cells were the most sensitive, with approximately 80% cell death in response to 1 μM arsenic trioxide. ML1 and K562GS cells were somewhat less sensitive with 20–30% cell death, whereas KCL22, THP1, HL60R and KG1 were largely resistant to the toxicity of 1 μM arsenic.

While there was no obvious correlation between arsenic sensitivity and the levels of basal NF-κB activity in the leukemia cells, inhibition of NF-κB potentiated significantly arsenic toxicity in a majority of the NF-κB-positive cells (Fig. 1C). Application of JSH-23, a specific NF-κB inhibitor, to the leukemia cells sensitized the NF-κB-positive ML1, K562GS, KG1, KCL22 and HL60R cells, resulting in a significant reduction of survival in response to arsenic. On the other hand, JSH-23 did not alter arsenic toxicity in NF-κB-negative THP-1 cells. In contrast, we found that JSH-23 did not potentiate arsenic toxicity in NB4 cells, which possessed low NF-κB activity and were already highly sensitive to arsenic, indicating that these cells' response to arsenic was independent of NF-κB. Based on these observations, we suggest that NF-κB confers resistance to arsenic in many, though not all, leukemia cells possessing active NF-κB.

3.2. Constitutive NF-κB activity contributes to elevated GSH in leukemia cells

Arsenic toxicity is mediated partly through the induction of reactive oxygen species (ROS) and GSH is the major cellular redox scavenger counteracting ROS [8;31;32]. To assess whether GSH may assist cell survival to arsenic challenge, we measured the intracellular GSH contents in the leukemia cells. The leukemia cells had different levels of GSH, ranging from 19 to 54 nmol/mg of protein (Fig. 2A). More importantly, there was an obvious inverse correlation between GSH levels and arsenic sensitivity (Figs 1B and 2A). The most sensitive NB4 cells had the lowest GSH levels; K562GS and ML1 cells, being somewhat less

sensitive, had intermediate GSH; whereas the arsenic resistant THP1, HL60R and KG1 had high GSH. Moreover, treatment of the leukemia cells with N-acetyl-L-cysteine to augment GSH significantly reduced arsenic toxicity in the sensitive NB4, K562GS and ML1 cells (Fig. 2B). These results support the conclusion that intracellular GSH protects the leukemia cells against arsenic toxicity.

We have recently shown that NF-κB signaling plays a crucial role in the maintenance of cellular GSH [7]. To test whether NF-κB was involved in GSH regulation in leukemic cells, we treated the NF-κB-positive leukemia cells with JSH-23 and measured GSH contents. JSH-23 caused a significant decrease of GSH in K562GS, KG1 and KCL22 (Fig. 2C); however, it did not affect GSH level in HL60R and NB4 cells. We suggest that constitutive NF-κB up-regulates GSH and confers resistance to arsenic in some leukemia cells.

3.3. Blocking NF-κB signaling reduces GSH via transcriptional downregulation of Gclc and Gclm expression in prostate cancer cells

Numerous lines of evidence indicate that NF-κB is constitutively active not only in blood cancers but also in solid tumors, including tissues from human patients with prostate cancer and in androgen-insensitive human prostate carcinoma cells [33]. To determine whether the NF-κB-GSH axis was effective also in prostate cancer cells, we first measured NF-κB activity in four lines of prostate cancer that differ in androgen-dependence, metastasis and invasiveness. Using a luciferase reporter assay, we detected different levels of basal NF-κB activities in these cells, with the lowest levels in LNCaP, higher in DU145 and PC3, and the highest in the highly metastatic PC-3MM2 (Fig. 3A). Treatment with the NF-κB inhibitor JSH-23 markedly reduced constitutive NF-κB activity in all prostate cancer cells examined. We next measured GSH contents and redox potentials. The prostate cancer cells had GSH levels ranging from 12 – 23 nmol/mg; correspondingly, they displayed different redox potentials with electronegative ΔE' values ranging from −135 to −150 mV (Fig. 3B). While JSH-23 significantly reduced GSH in the prostate cancer cells, it did not have such an effect in non-malignant fibroblasts and hPrEC cells, which were known to have low basal NF-κB activities [34] (Figs. 3B and 3C). Hence, as in leukemia cells, constitutively active NF-κB can increase GSH in prostate cancer cells.

We have previously shown that NF-κB signaling up-regulates GSH through transcriptional activation of the modifier and catalytic subunits of glutamine-cysteine ligase (GCL), the rate limiting enzyme for GSH biosynthesis [7]. To determine whether this was the case in prostate cancer cells, we examined the promoter activities of *Gclc* and *Gclm* in PC-3MM2 cells using gene-specific promoter-driven luciferase reporters. The activity of the *Gclc* promoter was markedly reduced and the activity of the *Gclm* promoter was moderately decreased by JSH-23 (Fig. 3D). Conversely, the activities of both promoters were induced significantly by *tert*-butylhydroquinone (tBHQ), an aromatic organic compound and a known GCL inducer. Based on these findings, we suggest that the active NF-κB may upregulate GCL expression, which in turn increases GSH biosynthesis in prostate cancer cells.

3.4. Pharmacological and molecular inhibition of the NF-κB signaling increases sensitivity to oxidative stress in prostate cancer cells

Because GSH plays a predominant role in the modulation of cellular redox balance, we asked whether NF-κB inhibition and subsequent GSH reduction would lead to higher reactive oxygen species (ROS). We treated PC-3MM2 cells with JSH-23 for 18 hours and measured H_2O_2-activated DCF fluorescence by flow cytometry (Fig. 4A). Compared to cells treated with control vehicle, 70% of cells treated with JSH-23 became DCF-positive (the M2 population in Fig. 4A). This effect of JSH-23 was even greater than that caused by the

strong oxidative stress inducer, hydrogen peroxide (H_2O_2), which induced 44% DCF-positive cells.

To test whether NF-κB inhibition could sensitize the cells to oxidative stress damage, we treated NF-κB-positive prostate cancer cells with JSH-23 and measured cell survival in the presence of H_2O_2 or arsenic trioxide. While JSH-23 was non-toxic for a short term usage, it exhibited a slight cytotoxicity when used for a longer time, perhaps due to inhibition of the pro-survival properties of NF-κB [6] (Figs. 4B and 4C). Nevertheless, pretreatment of cells with JSH-23 significantly potentiated the cytotoxicity of H_2O_2 and arsenic trioxide in all the prostate cancer cells (Figs. 4B and 4C). In the presence of JSH-23, the LC_{50} of H_2O_2 was reduced by 2–4 folds, whereas, that of arsenic trioxide was reduced by 1.5–3 folds (Tables 1 and 2). In contrast to its striking effect in prostate cancer cells, JSH-23 failed to further potentiate the toxicity of H_2O_2 and arsenic trioxide in the non-malignant prostate epithelial cells and fibroblasts (Figs. 4B and 4C). Hence, JSH-23 may be more selective to sensitize the prostate cancer cells to H_2O_2- and arsenic-induced oxidative damages.

JSH-23 is an aromatic diamine compound that may by itself affect cellular redox status. To evaluate the direct contribution of NF-κB signaling to redox modulation, we used siRNA to knockdown *IKK*β, the essential upstream kinase for NF-κB activation, in PC-3 MM2 cells. Compared to cells transfected with scrambled siRNA, cells transfected with *IKK*β siRNA had decreased *IKK*β mRNA and reduced GSH (Figs. 5A and 5B). When treated with arsenic, the cells transfected with *IKK*β siRNA displayed higher levels of DCF-labeling, indicating weaker reducing power and greater oxidative stress induction (Fig. 5C). Concurrently, the *IKK*β siRNA transfected cells were highly sensitive to arsenic, exhibiting much more annexin V-positive and TUNEL-positive apoptotic cells than those in control siRNA transfected cells (Fig. 5D). Taken the pharmacological and molecular NF-κB inhibition data together, we conclude that suppression of NF-κB signaling can down regulate glutathione, decrease redox potential and increase the sensitivity of prostate cancer cells to oxidative damage by arsenic.

4. Discussion

Constitutive NF-κB activation is found in approximately 15–20 % of all cancers [2;16]. In the present studies, we detect constitutive NF-κB activation in a number of leukemia and prostate cancer cells. We show that the constitutive NF-κB activity contributes to maintenance of cellular glutathione and redox potential in many “NF-κB positive” cancer cells, because inhibition of NF-κB by molecular and/or pharmacological means significantly reduces GSH.

Although NF-κB signaling has been proposed as a potential therapeutic target for molecular therapy to suppress tumorigenesis and enhance the efficacy of antineoplastic drugs, the molecular basis of the anti-NF-κB therapy is not fully understood [6;35]. Many chemotherapeutic agents, such as arsenic, act through the induction of oxidative stress that leads to cancer cell apoptosis [36–38]. GSH is an abundant thiol-containing small molecule that plays a crucial role in maintaining an intracellular reducing environment [8]. Based on our observations, it is possible that constitutive NF-κB activity in cancer cells contributes to higher GSH levels, thereby conferring stronger resistance to chemotherapy. Unlike the cancer cells, most non-malignant cells are known to have little, if any, basal NF-κB activities [34]. We show that neither inactivation of NF-κB affects the GSH content in normal prostate epithelial cells nor it sensitizes the cells to oxidative damage. Thus, inactivation of NF-κB and/or its upstream kinase IKKβ can reduce redox potential and potentiate the cytotoxicity of arsenic and H_2O_2 in many “NF-κB-positive” cancer cells.

NF-κB has been associated with several aspects of tumorigenesis. NF-κB can inhibit the expression of pro-apoptotic pathways, or induce anti-apoptotic gene expression and protein production [39], stimulate cytokine production thereby promoting the growth of both pre-malignant and formed tumors [16], induce angiogenesis via VEGF, IL-8, PDGF [40], and activate various cell cycle genes [41]. It has also been shown that NF-κB enhances the expression of the multidrug resistance (MDR) protein and mediates chemoresistance of tumor cells [42]. In this regard, results of this study are unique in revealing a novel role of NF-κB signaling in the regulation of glutathione that leads to the modulation of redox potential of cancer cells.

Human cancer is a highly heterogenous disease, with genetic and regulatory modules unique not only to different tumor types, but also to similar type tumors. This appears to be the case for NF-κB signaling in cancer cells. We show that NF-κB signaling is constitutively active in some, but not all, cancer cells. The active NF-κB contributes to elevate glutathione levels in some of the "NF-κB-positive" cancer cells, but does not affect glutathione in others. Furthermore, inhibition of NF-κB in HL60R leukemia cell does not affect glutathione but sensitizes HL60R to arsenic toxicity, indicating that constitutive NF-κB can promote HL60R cell survival through a mechanism independent of GSH. Based on these observations, we suggest that there are multiple mechanisms involved in glutathione regulation in cancer cells and that constitutive NF-κB activation is one of the factors contributing to elevated GSH. While further characterization of the regulatory mechanisms that generate heterogeneity is pertinent to understanding cancer-specific cell responses, our data indicate that constitutive NF-κB activity is one of the factors contributing to chemotherapeutic resistance. For a subpopulation of "NF-κB-positive" cancer cells, inhibition of NF-κB signaling may be combined with oxidative stress-based therapy to enhance the efficacy in cancer cell apoptosis.

Abbreviations

NF-κB	Nuclear Factor κB
GSH	glutathione
GCLC	Glutamine Cysteine Ligase Catalytic subunit
GCLM	Glutamine Cysteine Ligase Modifier subunit
ROS	Reactive Oxygen Species

Acknowledgments

This work is supported in part by Public Health Service grants from the National Eye Institute EY15227. We thank Dr. Shelly C. Lu for *Gclc*-Luc/*Gclm*-Luc plasmids, Alvaro Puga for critical reading of the manuscript and Yunxia Fan for technical assistance with FACS analyses.

References

1. Pahl HL. Activators and target genes of Rel/NF-kappaB transcription factors. Oncogene. 1999; 18:6853–6866. [PubMed: 10602461]
2. Pikarsky E, Porat RM, Stein I, Abramovitch R, Amit S, Kasem S, Gutkovich-Pyest E, Urieli-Shoval S, Galun E, Ben-Neriah Y. NF-kappaB functions as a tumour promoter in inflammation-associated cancer. Nature. 2004; 431:461–466. [PubMed: 15329734]
3. Pham CG, Bubici C, Zazzeroni F, Papa S, Jones J, Alvarez K, Jayawardena S, De SE, Cong R, Beaumont C, Torti FM, Torti SV, Franzoso G. Ferritin heavy chain upregulation by NF-kappaB inhibits TNFalpha-induced apoptosis by suppressing reactive oxygen species. Cell. 2004; 119:529–542. [PubMed: 15537542]

4. Chen F, Castranova V, Li Z, Karin M, Shi X. Inhibitor of nuclear factor kappaB kinase deficiency enhances oxidative stress and prolongs c-Jun NH2-terminal kinase activation induced by arsenic. Cancer Res. 2003; 63:7689–7693. [PubMed: 14633691]
5. Peng Z, Peng L, Fan Y, Zandi E, Shertzer HG, Xia Y. A critical role for IkappaB kinase beta in metallothionein-1 expression and protection against arsenic toxicity. J.Biol.Chem. 2007; 282:21487–21496. [PubMed: 17526490]
6. Luo JL, Kamata H, Karin M. IKK/NF-kappaB signaling: balancing life and death--a new approach to cancer therapy. J.Clin.Invest. 2005; 115:2625–2632. [PubMed: 16200195]
7. Peng Z, Geh E, Chen L, Meng Q, Fan Y, Sartor M, Shertzer HG, Liu ZG, Puga A, Xia Y. I{kappa}B kinase {beta} regulates redox homeostasis by controlling the constitutive levels of glutathione. Mol.Pharmacol. 2010
8. Meister A, Anderson ME. Glutathione. Annu.Rev.Biochem. 1983; 52:711–760. [PubMed: 6137189]
9. Sierra-Rivera E, Meredith MJ, Summar ML, Smith MD, Voorhees GJ, Stoffel CM, Freeman ML. Genes regulating glutathione concentrations in X-ray-transformed rat embryo fibroblasts: changes in gamma-glutamylcysteine synthetase and gamma-glutamyltranspeptidase expression. Carcinogenesis. 1994; 15:1301–1307. [PubMed: 7913422]
10. Guzman ML, Neering SJ, Upchurch D, Grimes B, Howard DS, Rizzieri DA, Luger SM, Jordan CT. Nuclear factor-kappaB is constitutively activated in primitive human acute myelogenous leukemia cells. Blood. 2001; 98:2301–2307. [PubMed: 11588023]
11. Barbarroja N, ristides-Torres L, Hernandez V, Martin C, Dorado G, Torres A, Velasco F, Lopez-Pedrera C. Coordinated deregulation of cellular receptors, proangiogenic factors and intracellular pathways in acute myeloid leukaemia. Leuk.Lymphoma. 2007; 48:1187–1199. [PubMed: 17577783]
12. Birkenkamp KU, Geugien M, Schepers H, Westra J, Lemmink HH, Vellenga E. Constitutive NF-kappaB DNA-binding activity in AML is frequently mediated by a Ras/PI3-K/PKB-dependent pathway. Leukemia. 2004; 18:103–112. [PubMed: 14574326]
13. Bueso-Ramos CE, Rocha FC, Shishodia S, Medeiros LJ, Kantarjian HM, Vadhan-Raj S, Estrov Z, Smith TL, Nguyen MH, Aggarwal BB. Expression of constitutively active nuclear-kappa B RelA transcription factor in blasts of acute myeloid leukemia. Hum.Pathol. 2004; 35:246–253. [PubMed: 14991544]
14. Suh J, Payvandic F, Edelstein LC, Amenta PS, Zong WX, Gelinas C, Rabson AB. Mechanisms of constitutive NF-kappaB activation in human prostate cancer cells. Prostate. 2002; 52:183–200. [PubMed: 12111695]
15. Palayoor ST, Youmell MY, Calderwood SK, Coleman CN, Price BD. Constitutive activation of IkappaB kinase alpha and NF-kappaB in prostate cancer cells is inhibited by ibuprofen. Oncogene. 1999; 18:7389–7394. [PubMed: 10602496]
16. Karin M, Greten FR. NF-kappaB: linking inflammation and immunity to cancer development and progression. Nat.Rev.Immunol. 2005; 5:749–759. [PubMed: 16175180]
17. Stephenson RA, Dinney CP, Gohji K, Ordonez NG, Killion JJ, Fidler IJ. Metastatic model for human prostate cancer using orthotopic implantation in nude mice. J.Natl.Cancer Inst. 1992; 84:951–957. [PubMed: 1378502]
18. Collins SJ, Robertson KA, Mueller L. Retinoic acid-induced granulocytic differentiation of HL-60 myeloid leukemia cells is mediated directly through the retinoic acid receptor (RAR-alpha). Mol.Cell Biol. 1990; 10:2154–2163. [PubMed: 1970118]
19. Tojima Y, Fujimoto A, Delhase M, Chen Y, Hatakeyama S, Nakayama K, Kaneko Y, Nimura Y, Motoyama N, Ikeda K, Karin M, Nakanishi M. NAK is an IkappaB kinase-activating kinase. Nature. 2000; 404:778–782. [PubMed: 10783893]
20. Yang H, Wang J, Ou X, Huang ZZ, Lu SC. Cloning and analysis of the rat glutamate-cysteine ligase modifier subunit promoter. Biochem.Biophys.Res.Commun. 2001; 285:476–482. [PubMed: 11444867]
21. Yang H, Wang J, Huang ZZ, Ou X, Lu SC. Cloning and characterization of the 5'-flanking region of the rat glutamate-cysteine ligase catalytic subunit. Biochem.J. 2001; 357:447–455. [PubMed: 11439094]

22. Senft AP, Dalton TP, Shertzer HG. Determining glutathione and glutathione disulfide using the fluorescence probe o-phthalaldehyde. Anal.Biochem. 2000; 280:80–86. [PubMed: 10805524]
23. Dalton TP, Chen Y, Schneider SN, Nebert DW, Shertzer HG. Genetically altered mice to evaluate glutathione homeostasis in health and disease. Free Radic.Biol.Med. 2004; 37:1511–1526. [PubMed: 15477003]
24. Melisi D, Chiao PJ. NF-kappa B as a target for cancer therapy. Expert.Opin.Ther.Targets. 2007; 11:133–144. [PubMed: 17227230]
25. Savickiene J, Treigyte G, Pivoriunas A, Navakauskiene R, Magnusson KE. Sp1 and NF-kappaB transcription factor activity in the regulation of the p21 and FasL promoters during promyelocytic leukemia cell monocytic differentiation and its associated apoptosis. Ann.N.Y.Acad.Sci. 2004; 1030:569–577. [PubMed: 15659839]
26. Kerbauy DM, Lesnikov V, Abbasi N, Seal S, Scott B, Deeg HJ. NF-kappaB and FLIP in arsenic trioxide (ATO)-induced apoptosis in myelodysplastic syndromes (MDSs). Blood. 2005; 106:3917–3925. [PubMed: 16105982]
27. Assef Y, Rubio F, Colo G, del MS, Costas MA, Kotsias BA. Imatinib resistance in multidrug-resistant K562 human leukemic cells. Leuk.Res. 2009; 33:710–716. [PubMed: 18977528]
28. Moon DO, Kim MO, Kang SH, Choi YH, Kim GY. Sulforaphane suppresses TNFalpha-mediated activation of NF-kappaB and induces apoptosis through activation of reactive oxygen species-dependent caspase-3. Cancer Lett. 2009; 274:132–142. [PubMed: 18952368]
29. Zhou GB, Li G, Chen SJ, Chen Z. From dissection of disease pathogenesis to elucidation of mechanisms of targeted therapies: leukemia research in the genomic era. Acta Pharmacol.Sin. 2007; 28:1434–1449. [PubMed: 17723177]
30. Wang ZY. Ham-Wasserman lecture: treatment of acute leukemia by inducing differentiation and apoptosis. Hematology.Am.Soc.Hematol.Educ.Program. 2003:1–13. [PubMed: 14633774]
31. Soignet SL. Clinical experience of arsenic trioxide in relapsed acute promyelocytic leukemia. Oncologist. 2001; 6 Suppl 2:11–16. [PubMed: 11331435]
32. Anderson ME. Glutathione: an overview of biosynthesis and modulation. Chem.Biol.Interact. 1998; 111–112:1–14.
33. Aggarwal BB, Shishodia S. Suppression of the nuclear factor-kappaB activation pathway by spice-derived phytochemicals: reasoning for seasoning. Ann.N.Y.Acad.Sci. 2004; 1030:434–441. [PubMed: 15659827]
34. Gasparian AV, Yao YJ, Kowalczyk D, Lyakh LA, Karseladze A, Slaga TJ, Budunova IV. The role of IKK in constitutive activation of NF-kappaB transcription factor in prostate carcinoma cells. J.Cell Sci. 2002; 115:141–151. [PubMed: 11801732]
35. Kim HJ, Hawke N, Baldwin AS. NF-kappaB and IKK as therapeutic targets in cancer. Cell Death.Differ. 2006; 13:738–747. [PubMed: 16485028]
36. Davison K, Mann KK, Miller WH Jr. Arsenic trioxide: mechanisms of action. Semin.Hematol. 2002; 39:3–7. [PubMed: 12012315]
37. Jing Y, Dai J, Chalmers-Redman RM, Tatton WG, Waxman S. Arsenic trioxide selectively induces acute promyelocytic leukemia cell apoptosis via a hydrogen peroxide-dependent pathway. Blood. 1999; 94:2102–2111. [PubMed: 10477740]
38. Miyajima A, Nakashima J, Yoshioka K, Tachibana M, Tazaki H, Murai M. Role of reactive oxygen species in cis-dichlorodiammineplatinum-induced cytotoxicity on bladder cancer cells. Br.J.Cancer. 1997; 76:206–210. [PubMed: 9231920]
39. Ravi R, Bedi A. NF-kappaB in cancer--a friend turned foe. Drug Resist.Updat. 2004; 7:53–67. [PubMed: 15072771]
40. Huang S, Robinson JB, Deguzman A, Bucana CD, Fidler IJ. Blockade of nuclear factor-kappaB signaling inhibits angiogenesis and tumorigenicity of human ovarian cancer cells by suppressing expression of vascular endothelial growth factor and interleukin 8. Cancer Res. 2000; 60:5334–5339. [PubMed: 11034066]
41. Guttridge DC, Albanese C, Reuther JY, Pestell RG, Baldwin AS Jr. NF-kappaB controls cell growth and differentiation through transcriptional regulation of cyclin D1. Mol.Cell Biol. 1999; 19:5785–5799. [PubMed: 10409765]

42. Bourguignon LY, Xia W, Wong G. Hyaluronan-mediated CD44 interaction with p300 and SIRT1 regulates beta-catenin signaling and NFkappaB-specific transcription activity leading to MDR1 and Bcl-xL gene expression and chemoresistance in breast tumor cells. J.Biol.Chem. 2009; 284:2657–2671. [PubMed: 19047049]

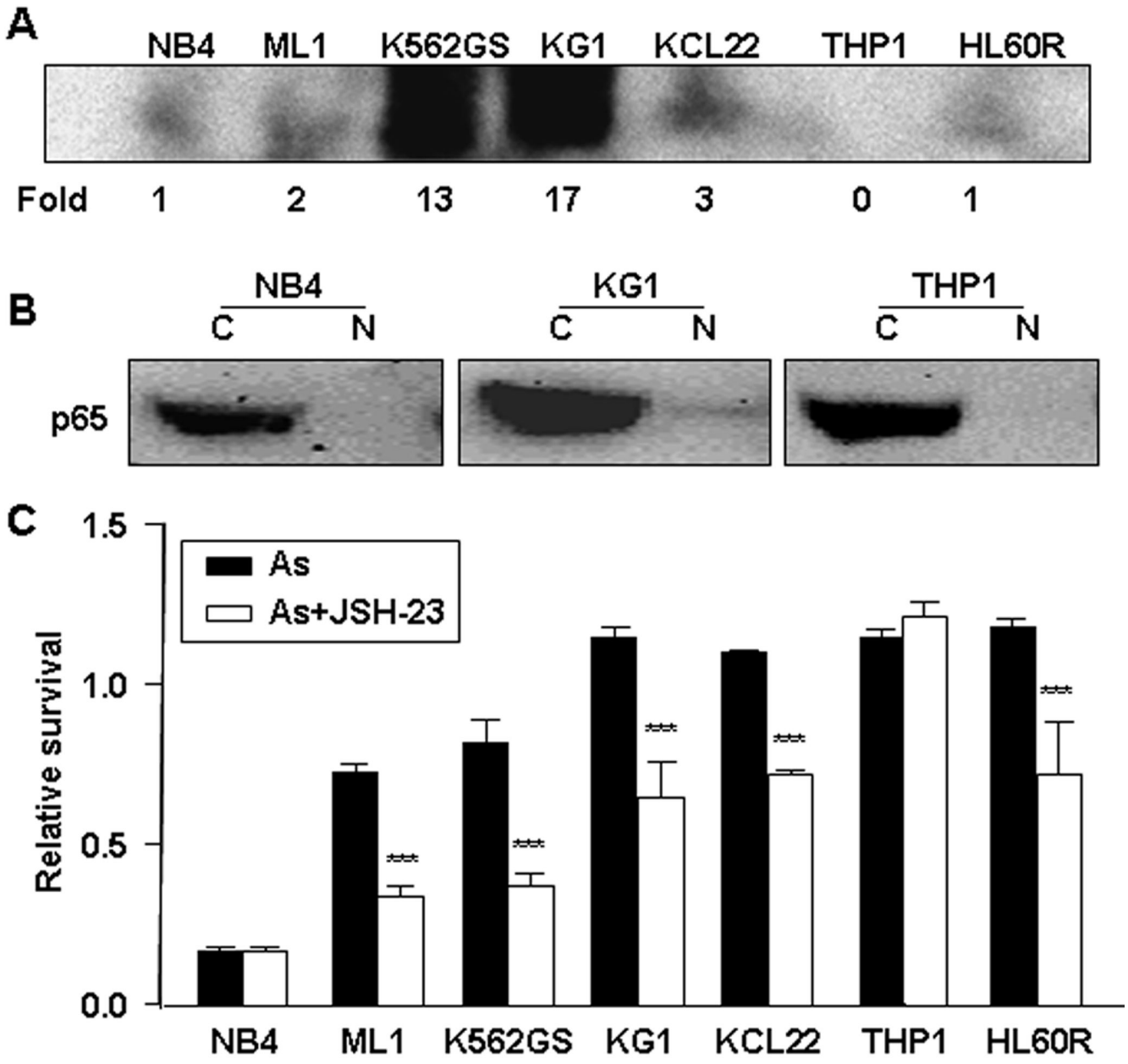

Figure 1. Constitutive NF-κB activity contributes to arsenic resistance in leukemia cells

The nuclear extracts isolated from various leukemia cell lines were used for (A) EMSA to determine NF-κB DNA binding activities, and (B) Western blotting to detect p-65. (C) Cells were treated with 1 μM arsenic trioxide in the presence and absence of JSH-23 for 3 days and evaluated viability by the MTS assay. Relative survival was calculated by comparison the MTS values of As treated versus untreated samples. The levels in untreated control and JSH-23 groups were designated as 1. Data are presented as the mean values ± S.E. from at least three independent experiments. Statistical analyses were performed based on the mean values in control and JSH-23 treated samples. ***$p < 0.001$ are considered statistically significant.

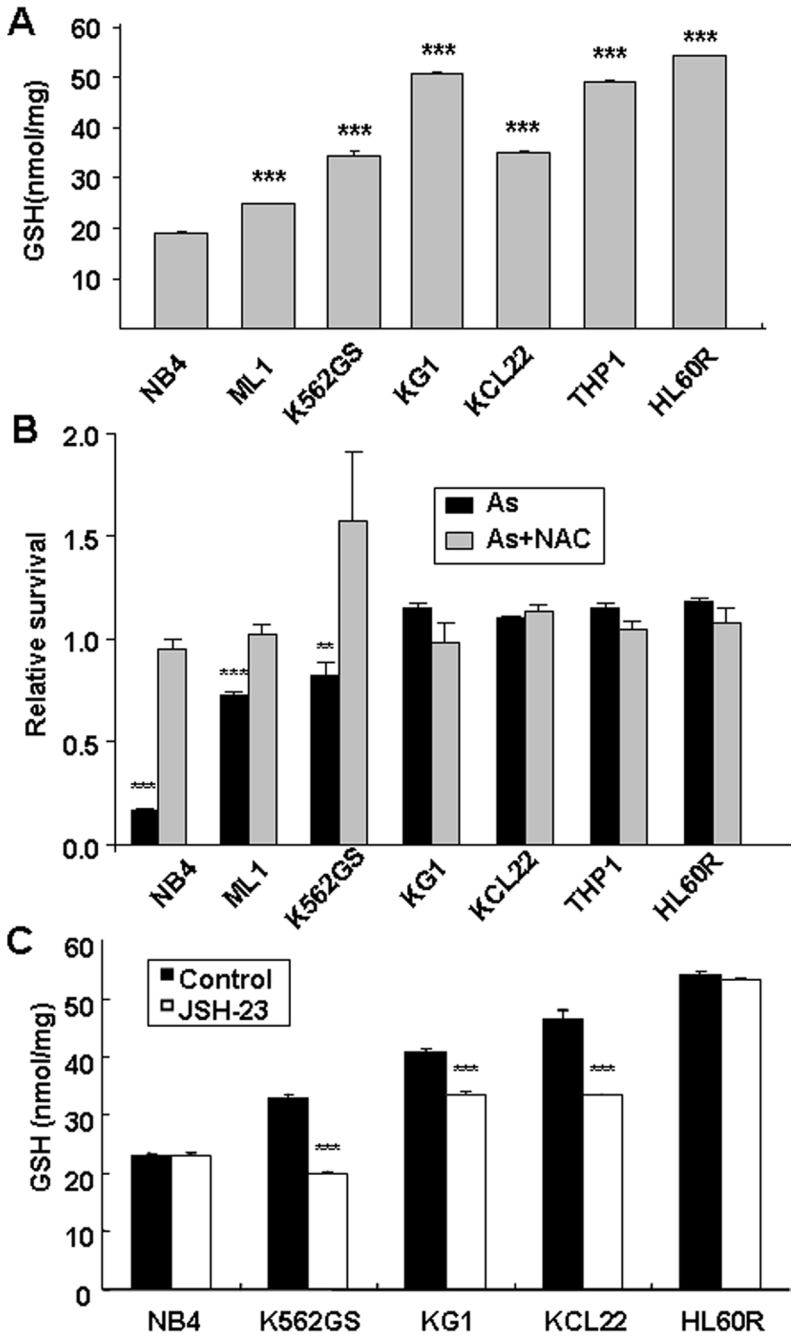

Figure 2. Inhibition of NF-κB reduces GSH in leukemia cells

The reduced glutathione GSH was measured in various leukemia cells in the absence (A and C) and presence (C) of the NF-κB inhibitor JSH-23 (10 μM) for 3 days. Statistical analyses of GSH in each sample were compared to the values in NB4 cells (A) and were based on the mean values in control and JSH-23 treated samples (C). (B) Leukemia cells were treated with 1 μM arsenic trioxide for 3 days in the absence and presence of NAC (5 mM). Cell viability was evaluated by the MTS assay. Relative survival and statistical analyses were calculated by comparison the MTS values of each cells without arsenic treatment. Data are presented as the mean values ± S.E. from at least three independent experiments. **p<0.01 and ***p<0.001 are considered statistically significant.

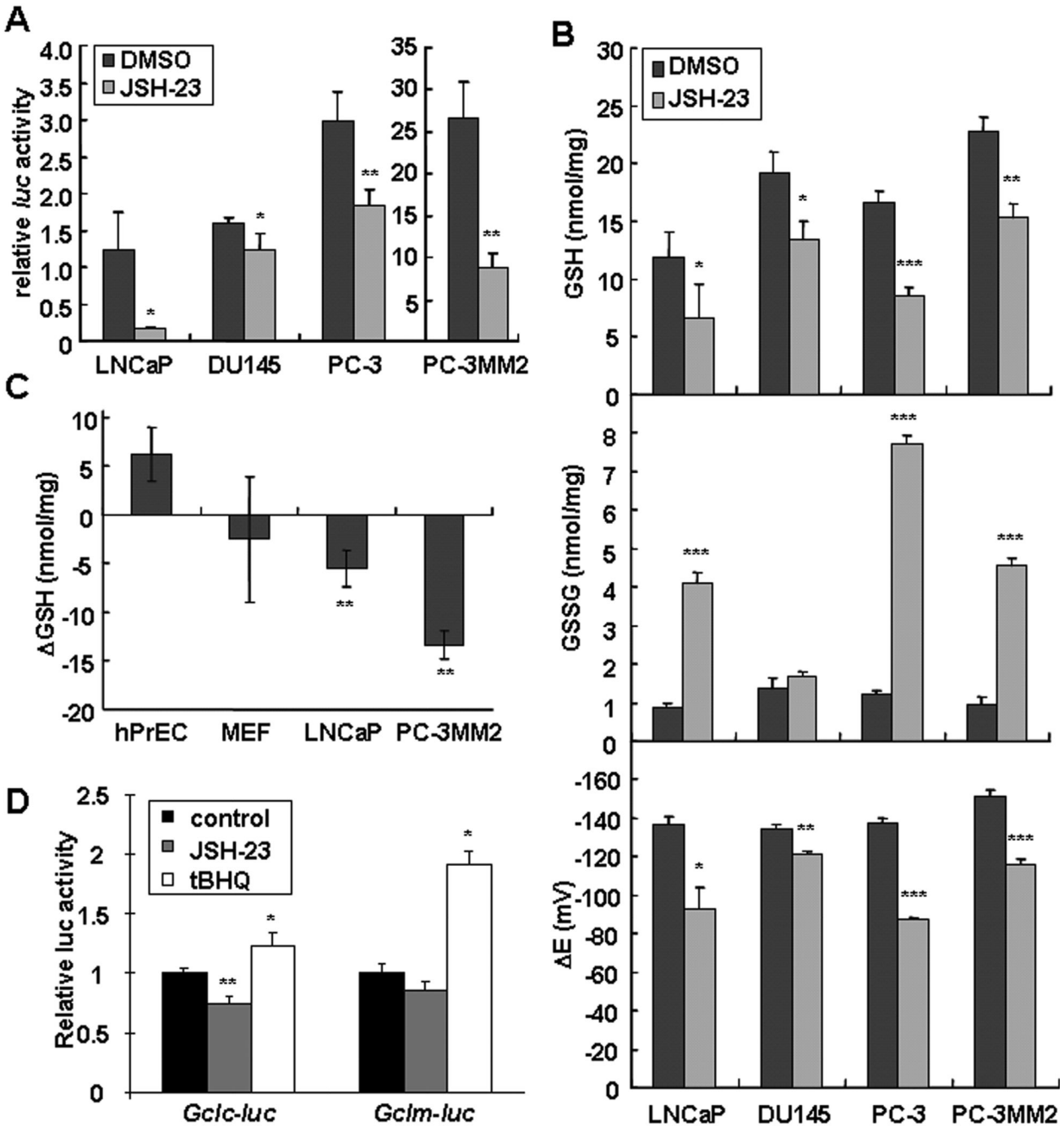

Figure 3. Inhibition of NF-κB reduces GSH and redox potential in prostate cancer cells

(A) The prostate cancer cells co-transfected with *NF-κB-luc* and *CMV-β-gal* plasmids were grown in medium in the presence and absence of the NF-κB inhibitor JSH-23 (100 μM). Relative luciferase activities were calculated based on β-gal values in each transfection, relative to the luciferase values in LNCaP cells designated as 1. Prostate cancer cells, hPrEC and MEF were maintained in the presence and absence of the NF-κB inhibitor JSH-23 (100 μM) for 24 hours. (B) Cellular GSH and GSSG were determined and redox potentials calculated in the prostate cancer cells. (C) Cellular GSH was determined in the cells as indicated, and the levels in JSH-23 cells were compared to that in the control DMSO-treated cells (ΔGSH). (D) The PC-3MM2 cells were transfected with *Gclc-luc* or *Gclm-luc* together

with the *CMV*-β-*gal* plasmids in the presence or absence of JSH-23 (100 μM) and tBHQ (10 μM) for 24 h. Relative luciferase activities were calculated based on β-gal values in each transfection. The luciferase values in cells not treated with chemicals were designated as 1. Data are presented as the mean values ± S.D. from at least three independent experiments. Statistical analyses were performed based on the mean values in treated versus untreated cells. * $p<0.05$, ** $p< 0.01$ and *** $p< 0.001$ are considered statistically significant.

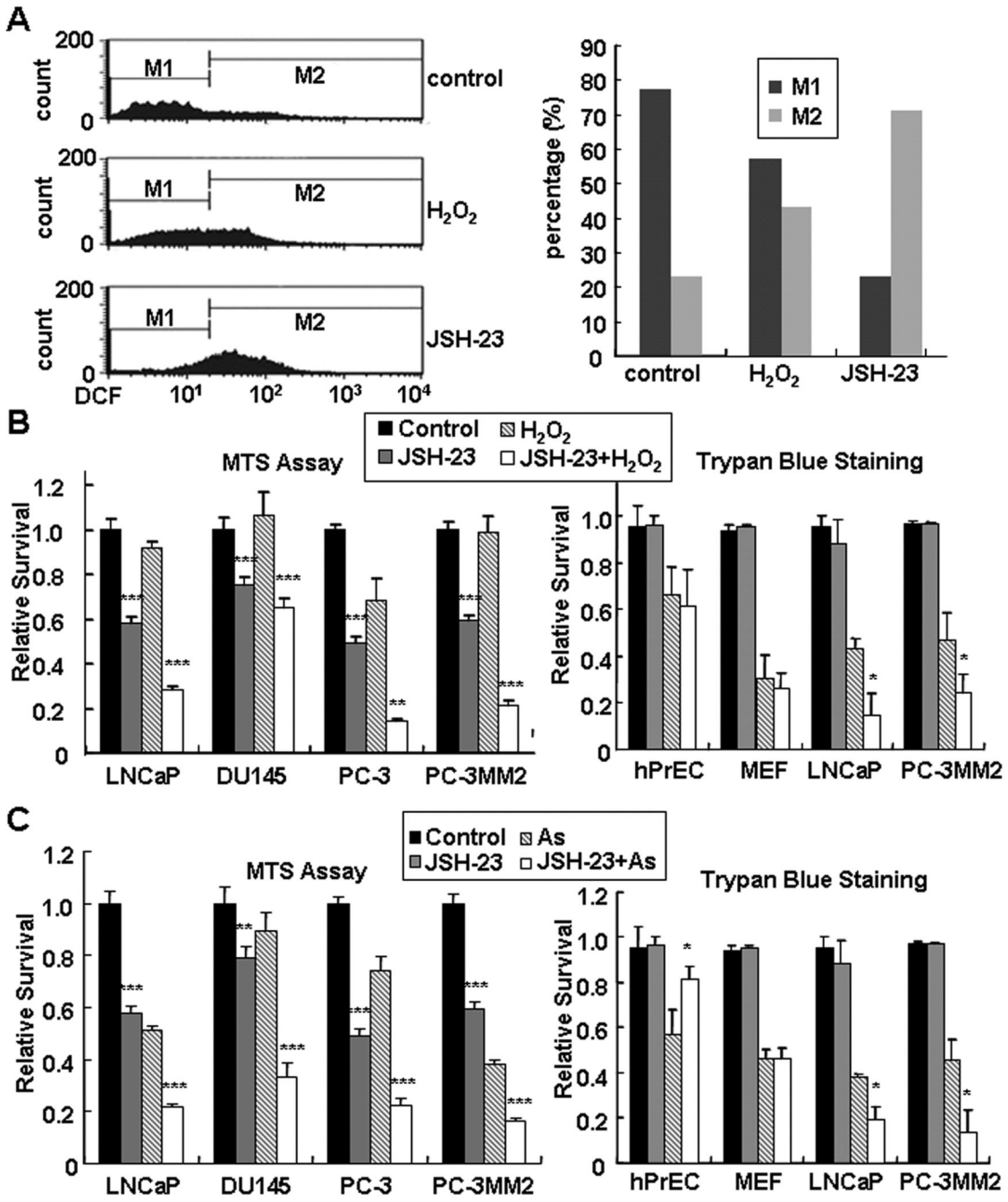

Figure 4. Pharmacological inhibition of the NF-κB signaling increases the susceptibility of prostate cancer cells to oxidative stress

(A) The prostate cancer cell line PC-3MM2 were either left untreated or treated with H_2O_2 (250 μM) for 2 h or JSH-23 (100 μM) for 18 h. Following CM-H_2DCFDA labeling, the DCF fluorescence intensity was quantified by flow cytometry and the "DCF-positive" (M2) and DCF-negative (M1) populations were quantified. The hPrEC, MEF and prostate cancer cells were treated with (B) H_2O_2 (250 μM) or (C) arsenic trioxide (62.5 μM). For MTS assays, the cells were treated for 12 h in the presence or absence of the NF-κB inhibitor JSH-23 (100 μM). The relative survival rates were calculated by comparison of the MTS values of H_2O_2 and As_2O_3 treated and untreated cells. Values in DMSO treated, but H_2O_2

and As_2O_3 untreated cells were designated as 1. For Trypan blue staining, the cells were treated for 30 min in the presence or absence of a 2 h JSH-23 (100μM) pretreatment. Results are presented as the mean values ± S.D. from at least three independent experiments. Statistically analyses were done by comparing the JSH-23 treated versus untreated samples under the same conditions. *$p< 0.05$, **$p<0.01$ and ***$p< 0.001$ are significant.

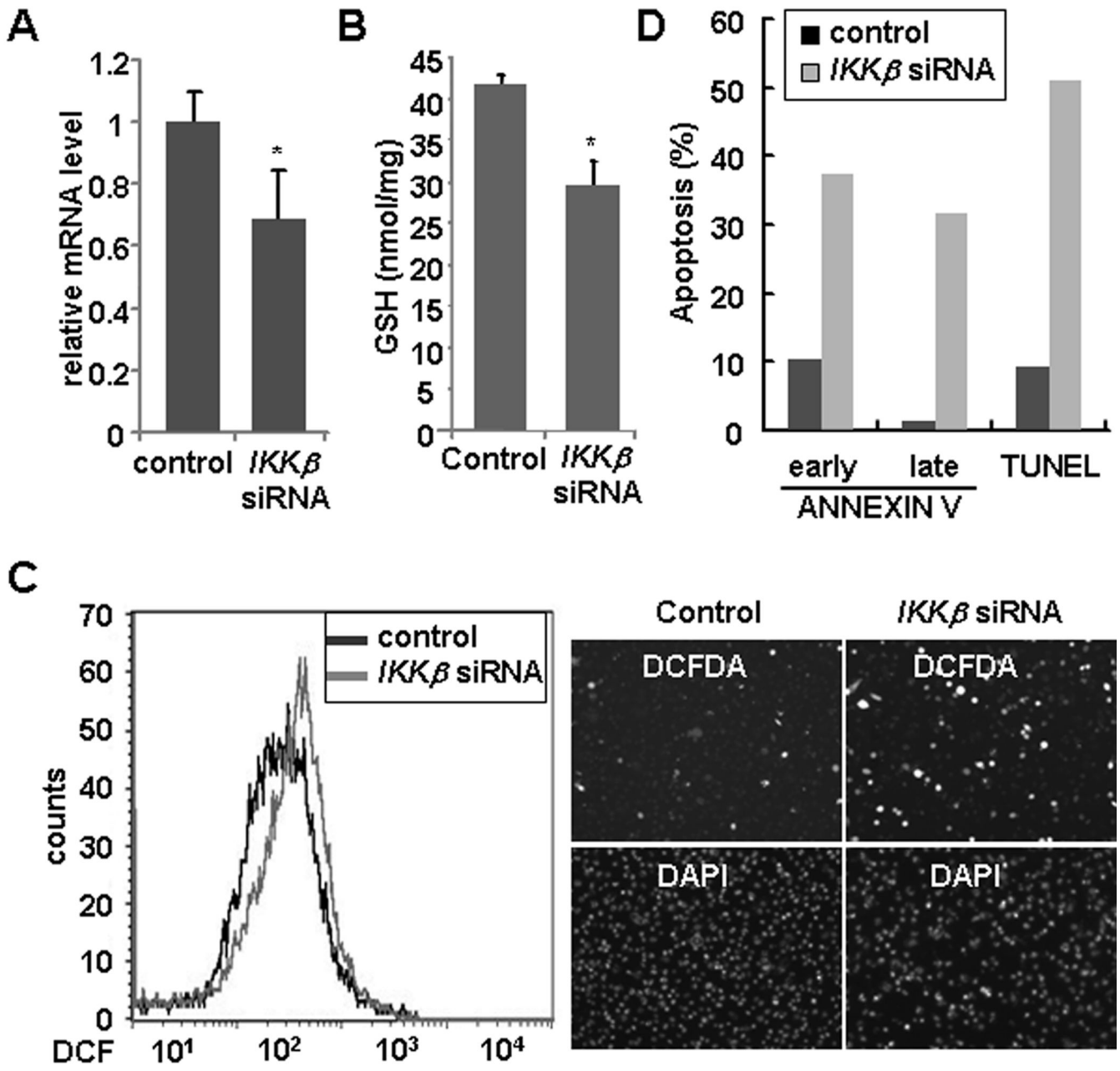

Figure 5. Molecular inhibition of the NF-κB signaling sensitizes prostate cancer cells to arsenic and oxidative toxicity

The PC-3MM2 cells were transfected with scrambled or *IKK*β siRNA for 48 h. (A) The relative *IKK*β mRNA level was determined by real-time PCR, adjusted to the GAPDH level as the loading control. IKKβ level in cells transfected with scramble siRNA was designated as 1, and (B) the cellular GSH level was measured. The transfected cells were treated with sodium arsenite (50 μM) for 6h. (C) Cells were labeled with CM-H_2DCFDA and the DCF-positive cells were identified by flow cytometry analysis (left panel) and fluorescent microscope (right panels). Cell apoptosis was determined by (D) Annexin V and TUNEL staining. The percentage of apoptosis was calculated by comparison to the values in control cells not exposed to arsenic. *p< 0.05, **p<0.01 and ***p< 0.001 are considered significant.

Table 1

LC_{50} of H_2O_2 in prostate cancer cells by MTS assays

Cell Lines	LC_{50} and 95% Interval H_2O_2 (μM)		p value
	Control	JSH-23 (100μM)	
LNCaP	613 (536, 700)	318 (254, 398)	2.5E-09
DU145	2426 (1877, 3134)	505 (454, 562)	1.1E-06
PC-3	344 (302, 392)	191 (0.26, 200)	6.7E-24
PC-3MM2	764 (673, 867)	102 (57, 185)	1.1E-19

Table 2

LC_{50} of arsenic trioxide in prostate cancer cells by MTS assays

Cell Lines	LC_{50} and 95% Interval As_2O_3 (μM)		p value
	Control	JSH-23 (100μM)	
LNCaP	110 (84, 169)	68 (48, 97)	2.5E-09
DU145	167 (118, 237)	47 (34, 65)	1.2E-08
PC-3	150 (107, 212)	102 (71, 144)	7.7E-12
PC-3MM2	64 (49, 84)	27 (19, 38)	1.2E-14